OFFICE OF NAVAL RESEARCH

Contract N00014-91-J-1078

R&T Code 4132046

Technical Report No. 39

THE EFFECT OF MELT PROCESSING CONDITIONS ON THE HYDROGEN-BONDED SHEET ORIENTATION AND POLARIZATION OF NYLON 11 FILMS

by S-L. Wu, J.I. Scheinbeim and B.A. Newman

Submitted
to
Special Edition of the Journal of Polymer Science, Polymer Physics Edition

Polymer Electroprocessing Laboratory
Department of Chemical and Biochemical Engineering
College of Engineering
Rutgers University
Piscataway, NJ 08855-0909

April 1996

The Effect of Melt Processing Conditions on the Hydrogen-bonded Sheet Orientation and Polarization of Nylon 11 Films

S-L Wu, J.I. Scheinbeim, and B.A. Newman
Polymer Electroprocessing Laboratory, College of Engineering
Rutgers -The State University of New Jersey
Piscataway, New Jersey 08855-0909

Synopsis

It is known that melt-quenched, cold-drawn, and then annealed nylon 11 films possess a particular doubly oriented hydrogen-bonded sheet structure: the hydrogen-bonded sheets being in the plane of the film and the molecular chain direction being in the direction of draw. In this study, nylon 11 was melted at 210°C in a hot press for different melting times (ranging from 30 seconds to 20 minutes) prior to quenching into an ice-water bath. The resulting orientation of the hydrogen-bonded sheet structure in these films following quenching, cold-drawing, and then annealing for the uniaxially drawn-annealed samples, and following quenching and then annealing for the undrawn-annealed samples, was examined using wide-angle x-ray diffraction and F.T.I.R spectroscopy. The results showed that for short times in the melt, films which are subsequently cold-drawn and then annealed exhibit a double orientation but as time in the melt increases, a change to a random orientation of the sheet structure about the draw (chain direction) is obtained. These results show that for melt quenched films with short times in the melt, a degree of preferred orientation of the hydrogen-bonded sheets in the plane of the film occurs. As time in the melt increases, the preferred orientation in the plane decreases. However, following cold drawing and several cycles of polarization using a maximum field of 150 MV/m at room temperature, the uniaxially drawn films processes from films with different times in the melt possessed the same final orientation of the hydrogen-bonded sheets in the film thickness direction and the same remanent polarization.

Introduction

In our laboratory, we discovered that melt-quenched and cold-drawn nylon 11,[1] and also other odd-numbered nylons[2], constitute a new class of ferroelectric polymers and that the piezoelectric response of nylon 11 is similar to that of poly(vinylidene fluoride) (PVF_2)[3] if we compare the response of each above their respective glass transition temperature, T_g. Northolt[4] discovered that initially melt-quenched, cold-drawn, and then annealed nylon 11 films possessed a doubly-oriented hydrogen-bonded sheet structure, with the molecular chains in the draw direction and the hydrogen-bonded sheets in the plane of the film. Upon polarizing an uniaxially drawn nylon 11 film, Scheinbeim *et al.*[5] found, based on the difference in the observed flat plate wide-angle x-ray diffraction patterns between unpoled and poled films, an initial 90° field-induced dipole reorientation (dipole switching), from the plane of the film to the film thickness direction, and then a 180° dipole reorientation for further switching cycles. This, of course, means that the hydrogen bonded sheet structure reoriented by 90° by simple rotation of the chains about their long axis.

In order to explain the double orientation for the melt-quenched, cold-drawn, and then annealed nylon 11 films, Northolt adopted the assumption proposed by Gordon[6] that hydrogen-bonded sheets were not broken up in the drawing process below the glass transition temperature T_g and therefore the regular stacking of the sheets resulted in a doubly-oriented hydrogen-bonded sheet structure in the plane of the film. However, the reason why uniaxially stretching at temperatures below T_g can result in a double orientation of melt-quenched nylon 11 films remained unclear. In the present study, we found that the time period spent in the melt, prior to quenching into an ice-water bath played an important role in whether or not a doubly oriented hydrogen-bonded sheet structure was obtained after cold drawing. In order to gain insight into the double orientation mechanism, orientation studies of the hydrogen-bonded sheet structure for melt-quenched nylon 11 films were carried out using wide angle x-ray diffraction (WAXD) and Fourier Transform Infrared (FTIR) studies. In addition, the effect of time in the melt on the subsequent ferroelectric response and polarization switching of the uniaxially drawn nylon 11 films was also investigated.

Experimental

Sample Preparation

Nylon 11 pellets used in this study were provided by Rilsan Corporation. These pellets were impacted into powder using a low temperature impactor from Spex Industries Inc.. The powder was dried overnight at 110°C in a vacuum oven, then sandwiched between aluminum foils in a hot press at 210°C, and pressed into thin films. The molten films were kept in the press for different period of times, ranging from 30 s to 20 m, and then quenched into an ice-water bath. Uniaxially drawn nylon 11 films were obtained by uniaxially stretching the melt-quenched films to a ratio of 3:1 with a speed of 0.08 mm/s at room temperature. The thickness of the uniaxially drawn films was ~20μm. To prepare uniaxially drawn-and poled nylon 11 films, uniaxially drawn films were evaporation coated with gold electrodes on opposing sides of the film, and then poled using a triangular electric waveform with a period of 640 s and maximum magnitude of 150 MV/m. A dry-air purge was applied during the poling process. Undrawn-annealed, uniaxially drawn-annealed, and uniaxially drawn-poled-annealed nylon 11 films were prepared by annealing at 180°C for 2 hours under high vacuum at a fixed film length.

X-ray Techniques

WAXD studies were carried out at room temperature using nickel-filtered CuKα radiation. WAXD scans were obtained using a Philips XRG 3100 X-ray Generator and vertical diffractometer. Flat-plate WAXD photographs (Statton Camera) were taken in 3 modes: end mode (incident x-ray beam along draw direction), edge mode (incident beam perpendicular to the draw direction and parallel to the plane of the film), and transmission mode (incident beam perpendicular to the draw direction and the plane of the film), as shown in Figure 1. CaF_2 powder was applied between the stacked nylon films to serve as an internal standard when the ***d***-spacings were determined. These spacings were indexed according to the unit cell dimensions proposed by Hasegawa *et al.*[7] From this model, nylon 11 crystals can be described by a triclinic α-form crystal structure with antiparallel chain packing.

FTIR Spectroscopy Measurements

FTIR spectra were obtained using a Digilab model FTS-60A FTIR spectrometer equipped with a TGS detector at a resolution of 2 cm^{-1}. A Perkin-Elmer wire grid polarizer was placed after the sample to collect the polarized spectra. The background and sample were scanned 200 times. A Balston dry air purge was used to remove atmospheric moisture. The thickness of the drawn films was in the range of 3.5 μm ~ 7 μm, which were thin enough to follow the Beer-Lambert Law.

Results

Effect of Time In the Melt on the Orientation of Hydrogen-Bonded Sheets in Uniaxially Drawn-Annealed Nylon 11 Films

Figure 2 shows the reflection mode WAXD scans for uniaxially drawn-annealed nylon 11 films with times in the melt of 30 s, 2 m, 5 m, 10 m, and 20 m. For the shortest melting time, a large peak (having a small shoulder), centered at $2\theta = 23°$, whose ***d***-spacing corresponds to the (020) planes from Hasegawa's model, is found. Since the X-ray diffracted intensities for the reflection mode scan results only from crystallographic planes in the plane of the nylon film, this suggests that the (020) plane, i.e. the crystallographic plane containing the hydrogen-bonded sheets, is in the plane of the film. This result was observed and reported by Northolt[4]. However, as time in the melt increases, the intensity of the second peak with a lower 2θ, centered at 20.9° whose ***d***-spacing corresponds to the (200) planes i.e. scattering from the crystallographic planes between hydrogen-bonded chains increases. This growth in the (200) intensity occurs at the expense of the (020) intensity and hence the (020) planes are no longer the only major set of crystallographic planes in the plane of the film. In order to quantitatively analyze the effect of melting time on the orientation of the (020) and (200) reflections in the plane of the film, each diffraction scan in Figure 2 was curve fitted by assuming:

1. The curve distribution for the amorphous regions and the (020) and (200) reflections can be characterized by Gaussian functions.[8]
2. The crystallinity of these uniaxially drawn-annealed nylon 11 films remains the same regardless of time in the melt.

3. The peak position for the (200) and (020) reflections is assumed fixed at 20.9° and 23° respectively, which was calculated from Hasegawa's model and confirmed from our flat plate wide-angle x-ray diffraction patterns, as shown in Figures 3-5.

Figure 3(a) shows the curve fitted result for uniaxially drawn-annealed nylon 11 films with time in the melt of 2 m. The area percentages of the (020) and (200) reflections of each diffraction scan were calculated after curve fitting and the results are shown in Figure 3(b), with respect to times in the melt. Results obtained from a single orientation of an oriented sample cannot reliably determine the percent crystallinity. However, we used these results to obtain a measure of crystallinity of ~46%. We note that this value is approximately the same as that found from trichroic infrared studies (~45%)[9]. If time in the melt for uniaxially drawn-annealed films is ~30 s, the area percentage for the (020) and (200) reflections is ~38% and ~8%, respectively. However, as time in the melt increases to ~20 m, the area percentage of the (020) reflection decreases and the area percentage of the (200) reflection increases to give values of 21% and 25%, respectively. This shows a gradual loss of double orientation (hydrogen-bonded sheets preferentially aligned in the plane of the film, and the chain axis in the draw direction) occurs with increasing time in the melt.

In order to confirm this loss of double orientation, flat-plate WAXD photographs were taken of these uniaxially drawn-annealed nylon 11 films. Figures 4 and 5 show the three diffraction modes, along with schematic representations of the observed diffraction patterns indexed according to Hasegawa's unit cell, for uniaxially drawn-annealed nylon 11 films with times in the melt of 30 s and 10 m, respectively. In these two figures, (a), (b), and (c) represent end, edge, and transmission modes, respectively. First, let's consider the films with time in the melt of 30 s. From the end mode photographs with the incident x-ray beam parallel to the draw direction, as shown in Figure 4(a), the reflections on the equatorial line are indexed as (020), which confirms that the hydrogen-bonded sheets are preferentially oriented in the plane of the film, and the other four reflections on the first layer line are indexed as (200). Hence, the crystallographic ***c***-axis is in the draw direction ($\boldsymbol{a}^* \times \boldsymbol{b}^* \,//\, \boldsymbol{c}$). Figure 4(b) shows the edge mode with the x-ray beam parallel to the ***a***-axis. The (020) reflection is observed on the equatorial line, as expected, and the

(00*l*) reflections are symmetrically disposed on either side of the meridian. Figure 4(c) shows the transmission mode with the incident beam parallel to ***b****. The (200) reflection appears on the equatorial line and the (00*l*) reflections on the meridional line. The unexpected presence of (00*l*) on the meridian was clarified by Mei[10] from the viewpoint of "stacking fault disorder". Second, for uniaxially drawn-annealed nylon 11 films with time in the melt of 10 m, the end mode, as illustrated in Figure 5(a), displays two concentric rings, indexed as (020) and (200) showing that the hydrogen-bonded sheets (020) reflection are now randomly disposed with respect to the draw direction. This is confirmed by the diffraction patterns of the edge and transmission modes, from Figures 5(b) and 5(c), respectively, which are found to be identical, and a superposition of the patterns of both edge and transmission modes for the uniaxially drawn-annealed films with time in the melt of 30 s. Combining the results from Figures 5(a), 5(b), and 5(c), we see that only a fiber texture along the draw direction is formed for uniaxially drawn-annealed nylon 11 films with a time in the melt of 10 m, i.e., the hydrogen-bonded sheets are randomly oriented about the draw (chain) direction. This result is consistent with that from the wide angle x-ray diffraction scans.

While the wide angle x-ray diffraction studies show a gradual loss of orientation of the hydrogen-bonded sheets about the chain axis direction for uniaxially drawn-annealed nylon 11 films with increasing time in the melt, FTIR spectra provide information on the role of both stretching and annealing on the loss of orientation. Figure 6 exhibits the typical FTIR spectrum of nylon 11 films. The band at ca. 3300 cm^{-1} is assigned to the hydrogen-bonded N-H stretching mode. Two strong bands at ca. 2920 and 2850 cm^{-1} are assigned to the antisymmetric and symmetric CH_2 stretching modes of the methylene groups, respectively. The band at ca. 1645 cm^{-1} is assigned to the Amide I mode, which is composed primarily of the carbonyl stretching motion (77-80%).[11,12] The band at ca. 1550 cm^{-1} is assigned to the Amide II mode and will not be discussed further in this paper. Figures 7 and 8 show the IR spectra of uniaxially drawn nylon 11 films with times in the melt of 30 s and 10 m, respectively. In these figures, (a) shows the N-H and CH_2 stretching mode regions and (b) shows the Amide I and Amide II mode regions. Each of these figures shows the spectra both parallel and perpendicular to the draw

direction, measured using polarized light positioned at 0° and 90° to the draw direction. The absorbance difference between the parallel and perpendicular directions is a result of chain alignment in the draw direction. The ratio of absorbance in the perpendicular direction to that in the parallel direction, $A_{\perp}/A_{//}$, of the N-H stretching, methylene stretching, and Amide I bands is shown on Table I. $A_{\perp}/A_{//}$ for the films with time in the melt of 30 s is found higher for all bands, compared to that for films with time in the melt of 10 m. Since the drawing process orients chains parallel to the draw direction, the transition dipole moment for the methylene groups (both symmetric and antisymmetric) and for the hydrogen-bonded amide groups is approximately in the plane transverse to the chain direction. The higher $A_{\perp}/A_{//}$ values on these bands for uniaxially drawn films with time in the melt of 30 s suggests that more amide and CH_2 groups are detected in the direction perpendicular to the chain and in the plane of the film, while the lower $A_{\perp}/A_{//}$ for samples with time in the melt of 10 m implies some groups move away from the plane of the film towards the thickness direction. Hence, nylon 11 films with times in the melt of 30 s have a higher degree of orientation after stretching for the amide and methylene groups in the plane of the film than those with time in the melt of 10 m. This indicates uniaxially drawn nylon 11 films with time in the melt of 30 s show the pre-existence of a doubly oriented structure before annealing, while those with time in the melt of 10 m show much less order.

Next, let us consider the effect of annealing on the uniaxially drawn nylon 11 films. Figures 9 and 10 show the IR spectra of uniaxially drawn nylon 11 films with time in the melt of 30 s and 10 m, respectively, with the polarizer in the direction perpendicular to the draw direction. Figures 9(a) and 10(a) show N-H and CH_2 stretching bands and (b) shows Amide I and Amide II bands. Each of these figures shows the bands before and after the annealing process. The half width of the N-H stretching and Amide I bands decreases after annealing for both samples which implies that the strength of the hydrogen-bonded amide groups becomes more uniform. In addition, after annealing, the peak intensity of the N-H stretching band for the uniaxially drawn films with time in the melt of 30 s increases by 75% and that of the Amide I band increases by 50%, as shown

on Figure 9, while peak intensities of both bands for the samples with time in the melt of 10 m show only minor increases, as shown in Figure 10. For uniaxially drawn films with time in the melt of 30 s, the increase in peak intensities for the N-H stretching and Amide I bands indicates that the net dipole moment of the hydrogen-bonded amide groups is enhanced in the plane of the film and perpendicular to the draw direction. The increased band of intensities caused by the annealing process probably result from:

1. Increase of crystallinity:

   Skrovanek *et al.*[13] confirmed that the Amide I band is conformationally sensitive and attributed it to the hydrogen-bonded carbonyl groups in ordered and disorder regions and free carbonyl groups. As shown in Figure 9(b), the peak frequency of the Amide I band shifts from 1640 cm^{-1} to 1637 cm^{-1} after the annealing treatment and, combined with the intensity increase, suggests that the area of the ordered regions grows at the expense of that of the free and disordered regions. The crystallization process introduces more chains into the crystalline regions which maintain the doubly oriented texture which has already occurred.

2. Closer packing of the hydrogen-bonded sheets in the plane of the nylon film:

   Yu *et al.*[9] confirmed, using trichroic infrared studies, that the average amide plane orientation moves toward the plane of the film in the annealing process. Lee *et al.*[14] found that the ***d***-spacing for the (020) reflection decreases from 4.21 to 3.88 Å in the annealing process. This closer packing of the hydrogen-bonded sheets enhances the intensity of the amide bands. The closer packing of the sheets may also enhance the degree of order of the methylene groups in the sheet and, therefore, the peak intensity of the symmetric CH_2 stretching band is enhanced, as illustrated in Figure 9(a).

Even though closer packing of the hydrogen-bonded sheets also occurs for uniaxially drawn films with time in the melt of 10 m, the lesser degree of orientation obtained for the amide groups after the stretching process, compared to films with time in the melt of 30 s, does not give rise to an increase in the peak intensity after the annealing process for the two bands in the direction perpendicular to the chain.

As previously discussed, the degree of double order of the amide groups in stretched nylon 11 films decreases with increasing time in the melt. This implies melt-

quenched nylon 11 films with different times in the melt may have different orientations and perhaps also different morphologies before the stretching process occurs, either in the crystalline or the amorphous regions or in both. Wide angle x-ray diffraction studies were performed on undrawn-annealed nylon 11 films with two different times in the melt. Figures 11 and 12 show the edge (or end) and transmission modes, along with schematic representations of the observed diffraction patterns indexed according to Hasegawa's unit cell, for undrawn-annealed nylon 11 films with times in the melt of 30 s and 10 m, respectively. These diffraction patterns of both edge and transmission modes for both samples show two concentric rings, which are indexed as the (200) and (020) reflections. Moreover, if we examine the (020) reflection in edge mode for both films in more detail, we find that the intensity around the equatorial region is higher than that around the meridional region. This indicates that the hydrogen-bonded sheets for both films show a degree of preferred orientation in the plane of the film even before stretching. This result appears to play an important role in the process by which the melt-quenched, cold-drawn, and then annealed nylon 11 films obtain their doubly-oriented hydrogen-bonded sheet structure, as shown in past studies[4]. However, the reason why uniaxially drawn nylon 11 films processed from films with times in the melt of 10 m lose the doubly-oriented sheet structure remains somewhat unclear, because both films with different times in the melt exhibit a degree of preferred orientation of the hydrogen-bonded sheets in the plane of the film. In order to further examine the effect, WAXD scans were taken on undrawn-annealed films with times in the melt of 30 s and 10 m and the results are shown in Figure 13. This figure also shows the curve fitted results from each diffraction scan using the same assumptions previously used for the uniaxially drawn-annealed samples. The area percentages were calculated and the results are shown in Table II. The ratio of the area percentage of the (020) reflection to that of the (200) reflection, for time in the melt of 30 s is ~2.2, whereas the same ratio for time in the melt of 10 m is ~1.56. This indicates a preferred orientation of the hydrogen-bonded sheets already existed for both the undrawn-annealed nylon 11 films with different times in the melt, as shown in Figures 11 and 12. However, as time in the melt increases, the area percentage of the (200) reflection increases at the expense of that of the (020) reflection. This shows that the degree of

orientation of the hydrogen-bonded sheets in the plane of the film becomes less with increasing time in the melt. This result may be the important factor in explaining why melt-quenched nylon 11 films with long times in the melt which are subsequently uniaxially drawn and annealed lose their doubly oriented structure.

While WAXD studies on undrawn-annealed nylon 11 films show a degree of preferred orientation of the hydrogen-bonded sheets in the plane of the film, IR studies can also provide information on the orientation of hydrogen-bonded amide groups before and after annealing. Figures 14 and 15 show the IR spectra of melt-quenched nylon 11 films with times in the melt of 30 s and 10 m, respectively. In these figures, part (a) shows the N-H and CH_2 stretching bands and part (b) shows the Amide I and Amide II bands. Each figure shows the bands before and after annealing. The peak intensity for the N-H stretching and Amide I bands increases by 60% and 40%, respectively, for the samples with time in the melt of 30 s and by 50% and 30% for those with time in the melt of 10 m after annealing. The intensity increases with annealing observed for both types of samples are more similar to the uniaxially drawn-annealed nylon 11 films made from melt-quenched films with time in the melt of 30 s than to those with time in the melt of 10 m as shown in Figures 9 and 10. This again suggests a degree of preferred orientation of the hydrogen-bonded sheets in the plane of the film exists before stretching. Moreover, as time in the melt increases, the ratio of peak intensities from the annealing treatment for both N-H stretching and Amide I bands decreases, which suggests that the preferred orientation of hydrogen-bonded sheets in the plane of the film decreases with time in the melt. These results are consistent with those obtained from wide-angle x-ray diffraction studies. In conclusion, undrawn nylon 11 films with times in the melt of 30 s and 10 m both have preferred orientation of the hydrogen-bonded sheets in the plane of the film; however, the samples with time in the melt of 30 s have significantly greater orientation than those with time in the melt of 10 m.

Effect of Melting Time on Ferroelectric Properties and Polarization Mechanism for Uniaxially Drawn Nylon 11 Films

Figures 16(a) and (b) show the current density, $\boldsymbol{J}$, and electric displacement, $\boldsymbol{D}$, as a function of electric field, $\boldsymbol{E}$, respectively for uniaxially drawn nylon 11 films with times

in the melt of 30 s and 10 m. To enhance the degree of reproducibility, an aluminum spacer was used to prepare melt-quenched films of uniform thickness. The thickness of the resulting drawn nylon 11 films is ≈20 μm with an accuracy of ±0.3 μm. The remanent polarization, P_r, equal 51.7 and 51 mC/m^2 and the coercive field, E_c, equals 56.1 and 57.2 MV/m for samples with times in the melt of 30 s and 10 m, respectively. Since the percentage difference of both P_r and E_c falls within 2% and the half-width and peak height of the J vs E curves are the same for samples with different melting times, the ferroelectric response of the nylon 11 films remains identical despite different times in the melt before quenching and cold drawing.

Figures 17 and 18 each show all three diffraction modes, along with schematic representations of the observed reflections, from the flat-plate WAXD photographs of uniaxially drawn-poled-annealed nylon 11 with time in the melt of 30 s and 10 m, respectively. The diffraction patterns are similar when comparing the same diffraction mode between the two samples. Figures 17(a) and 18(a) both show end mode with (020) reflections on the meridian. This implies that during electric field poling, the hydrogen-bonded sheet orientation is switched about the c-axis to the film thickness direction irrespective of the initial orientation of the sheets before poling. For uniaxially drawn nylon 11 film with time in the melt of 30 s, the (020) planes are switched 90° from the plane of the film to the film thickness direction after poling, as shown in the end mode diffraction patterns of Figures 4(a) and 17(a); a double orientation remains but with a 90° reorientation of the chains about the c-axis with respect to their initial orientation. This can also be verified from the fact that the diffraction pattern in the edge mode for uniaxially drawn-poled-annealed nylon 11 films, as shown in Figure 17(b), is similar to that of the transmission mode for uniaxially drawn-annealed films, as shown in Figure 4(c), and the diffraction pattern in transmission mode for the uniaxially drawn-poled-annealed films, as shown in Figure 17(c), is similar to that of the edge mode for uniaxially drawn-annealed films, as shown in Figure 4(b), where the diffraction pattern for the edge mode is obtained by physically rotating the films 90° about the c-axis (draw) direction from the transmission mode and vice versa. This result is consistent with the polarization mechanism proposed by Scheinbeim *et al.*[5] For uniaxially drawn nylon 11

films made from melt-quenched films with time in the melt of 10 m, the poling treatment gives rise to a three-dimensional texture with the hydrogen-bonded sheets perpendicular to the plane of the film, as shown in Figure 18, which is produced from film with fiber texture. The same diffraction pattern occurs after poling for uniaxially drawn nylon 11 films with the two different times in the melt. In both cases, dipoles in hydrogen-bonded sheets, either in the plane of the film or randomly distributed about the ***c***-axis, are switched toward the film thickness direction upon electric field poling and consequently the ferroelectric response for both films is identical after the first poling cycle.

Discussion

As previously shown, melt-quenched nylon 11 films have a preferred orientation of the hydrogen-bonded sheets in the plane of the film. It is reasonable to believe that, even before quenching into an ice-water bath, a preferred orientation of the sheets in the melt already exists during the pressing process. This was confirmed by Besseler *et al*[15] which showed that the chain configurations in the melt are restricted in polyamides and thus hydrogen-bonded sheets are hardly broken in the melt state. Based on this result, Itoh[16] and Mei *et al.*[2] were then able to explain the fact that the higher melting temperatures observed for the nylon series, compared to polyethylene, a pure hydrocarbon, occurs because of the low melt entropy resulting from the hydrogen-bonded sheets persisting in the melt. While melt-pressing nylon 11 powder into film, shear stress results in the hydrogen-bonded sheets flowing out in all directions along the plane of the pressing plate. During subsequent melt-quenching of the film, the preferred orientation of the hydrogen-bonded sheets in the plane of the film is maintained.

The next question to address is why uniaxially drawn films made from felt-quenched films with short times in the melt exhibit a double orientation and, as time in the melt increases, these films exhibit more of a fiber pattern. As we have seen, films with short time in the melt have preferred orientation of the hydrogen-bonded sheets in the plane of the film, and as time in the melt increases, the preferred orientation gradually decreases. This preferred orientation is obviously the most important factor in determining whether or not we obtain a doubly oriented structure on drawing. In

addition, as the hydrogen-bonded sheets flow out radially in the melt under shear, amide groups other than those in the sheet may be carried by the sheet and, therefore, the relaxation time for these free amide groups may possibly play another critical factor in determining the degree of double orientation obtained. These free amide groups may form pseudo sheets or random coils, depending upon whether or not the time in the melt is long enough for them to relax. The quench process maintains to some degree the performed orientation existing in the melt. During the stretching process which follows, the films enhance both orientation and crystallinity. From the IR spectra, the ratio $A_{\perp}/A_{//}$ of the hydrogen-bonded amide groups of undrawn films is 1 and for uniaxially drawn films is 5 and 1.8, for times in the melt of 30 s and 10 m, respectively. From WAXD scans, the crystallinity is 32% and 46% for undrawn-annealed films and uniaxially drawn-annealed films respectively. Therefore, as the drawing process proceeds, not only do the hydrogen-bonded sheets adjust their orientation so that main chains are parallel to the draw direction but also more amide groups from the amorphous region come in to register with other amide groups and form hydrogen-bonded sheets in the growing crystalline regions. Nylon 11 films with a short time in the melt have a preferred orientation of hydrogen-bonded sheets in the plane of the film before stretching. As the crystalline regions are reoriented to the direction of draw upon stretching, amide groups in hydrogen-bonded sheets can easily form hydrogen bonds with neighboring groups in the amorphous region with a "pseudo" sheet form without reorienting these sheets out of the plane of the film and, therefore, the drawn sample possesses a doubly-oriented sheet structure. On the other hand, as time in the melt increases, the hydrogen-bonded sheets of the undrawn films become less ordered in the plane of the film. During stretching, these hydrogen-bonded sheets find greater difficulty in maintaining their orientation in the plane of the film as reorientation of the crystalline regions and the coming into register of amide groups from amorphous regions with a more random orientation takes place and this results in more of a fiber orientation.

After the drawing process, the chains are aligned in the draw direction and dipoles are in the plane perpendicular to the draw direction, regardless of the time in the melt. Scheinbeim *et al.*[5] proposed an initial 90° field-induced dipole orientation and then a 180°

dipole reorientation for further cycles when polarizing uniaxially drawn nylon 11 films with a doubly-oriented sheet structure. This means that the dipoles within the sheet respond to the applied electric field by switching from the plane of the film to the film thickness direction. The results also show that the ferroelectric response and flat-plate wide-angle x-ray diffraction patterns for uniaxially drawn nylon 11 films after polarization are the same regardless of the time period in the melt. We are then led to the fact that upon polarization the ability of dipoles to rotate out of a sheet is independent of whether the amide groups are in the plane of the film or not, and are able to switch into the applied electric field direction. This implies initial polarization switching mechanisms in addition to the proposed 90° rotation[17].

Conclusions

Based on the results of our studies of melt-quenched and undrawn-annealed nylon 11 films, and melt-quenched uniaxially drawn-annealed, and melt-quenched uniaxially drawn-poled-annealed nylon 11 films, using both WAXD and infrared spectroscopic studies, the following conclusions are reached:

1. The process of melt pressing nylon 11 films results in a shear induced flow producing a preferred orientation of hydrogen-bonded sheets in the plane of the pressed film.
2. Undrawn-annealed nylon 11 films with different times in the melt before quenching showed a degree of preferred orientation of the hydrogen-bonded sheets in the plane of the film. As time in the melt increased, the orientation of the hydrogen-bonded sheets in the plane of the film decreased. This, we believe, is the important factor in determining whether or not a doubly-oriented sheet structure is obtained after cold-drawing and annealing.
3. As time in the melt before quenching nylon 11 films into an ice-water bath increased, the degree of double orientation obtained by cold drawing and annealing the films decreased. At long times in the melt (~10 minute) for the melt-pressed films, a fiber orientation is obtained on subsequent cold-drawing, i.e., random hydrogen-bonded sheet orientation about the draw direction.

4. Even though uniaxially drawn nylon 11 films made from melt-quenched films with longer time in the melt lost the double orientation structure, dipoles in these films still switched into the film thickness direction after poling and the ferroelectric response after several poling cycles was identical to films with much shorter times in the melt, i.e. P_r, the remanent polarization, and E_c, the coercive field, were the same regardless of the time in the melt before quenching.

Work supported in part by CAFT (Rutgers) and ONR.

Table I

$A_{\perp}/A_{//}$ of N-H Stretching, Methylene Stretching, and Amide I Bands for Uniaxially Drawn Nylon 11 Films with Times in the Melt of 30 s and 10 m

Time in the melt	$A_{\perp}/A_{//}$			
	N-H stretching	Amide I	CH_2-antisymmetric	CH_2-symmetric
30 s	5	5.1	2.6	2.8
10 m	1.8	1.8	1.5	1.6

Table II

The Area Percentage of (020) and (200) Reflections for Unoriented- Annealed Nylon 11 Films with Times in the Melt of 30 s and 10 m

Time in the melt	Area percentage for (020)	Area percentage for (200)	Ratio
30 s	21.8	9.9	2.2
10 m	19.1	12.2	1.56

(a) End Mode

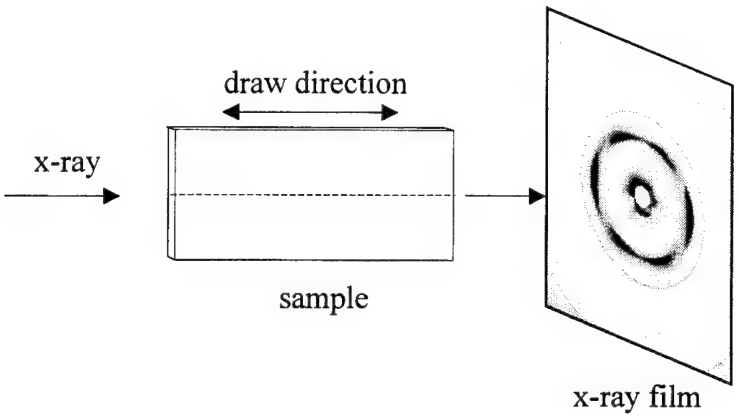

(b) Edge Mode

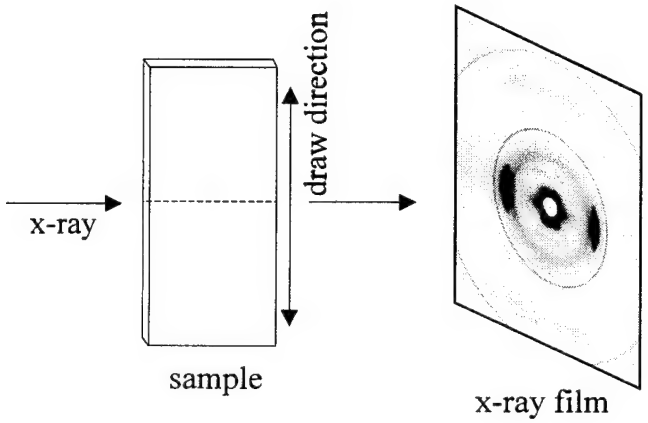

(c) Transmission Mode

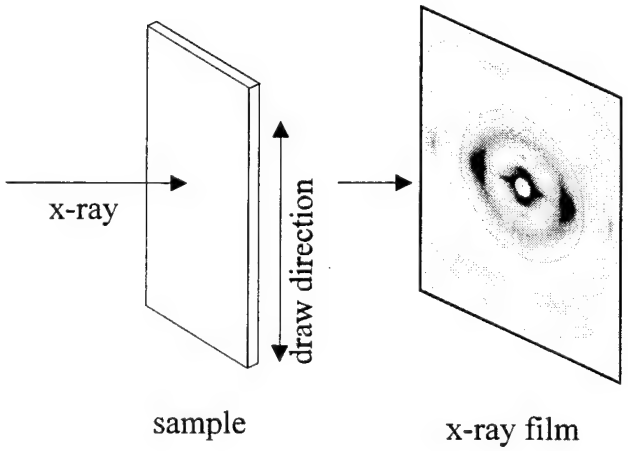

Figure 1 Orientation of nylon 11 film with respect to x-ray incident beam direction in the flat plate wide-angle x-ray diffraction study. The diffraction patterns shown were taken on uniaxially drawn-annealed nylon 11 films.

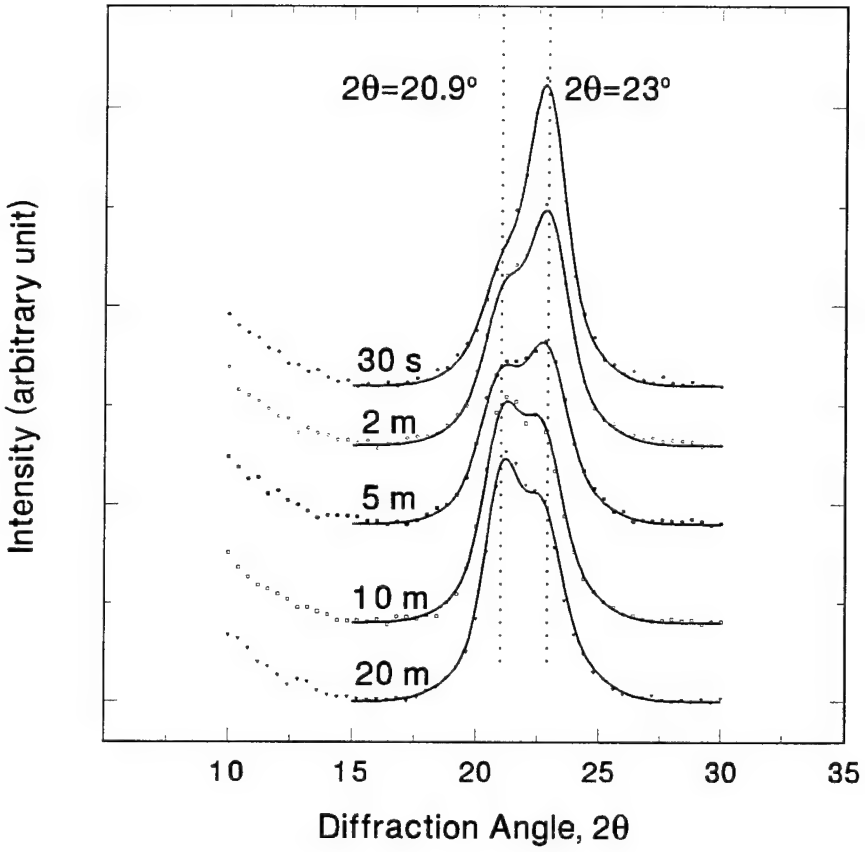

Figure 2 Wide-angle x-ray diffraction scans for uniaxially drawn-annealed nylon 11 films with times in the melt of 30 s, 2 m, 5 m, 10 m, and 20 m. The scans were taken in reflection mode.

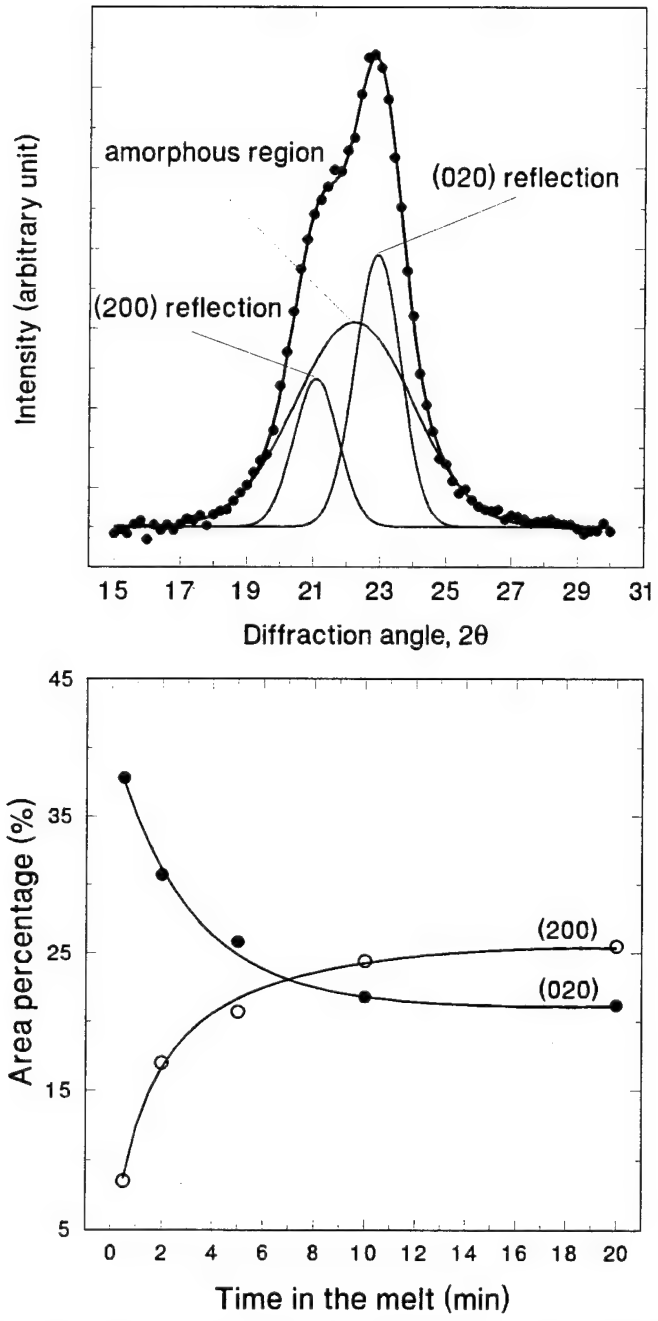

Figure 3 (a) shows the curve fitted result for uniaxially drawn-annealed nylon 11 films with time in the melt of 2 m. The bold solid line is the resultant curve obtained by summing the curves of the amorphous region and the (200) and (020) reflections. (b) shows the area percentage of the (020) and (200) reflections for uniaxially drawn-annealed nylon 11 films versus time in the melt. The area percentages were calculated after curve fitting each diffraction scan.

(a) End Mode

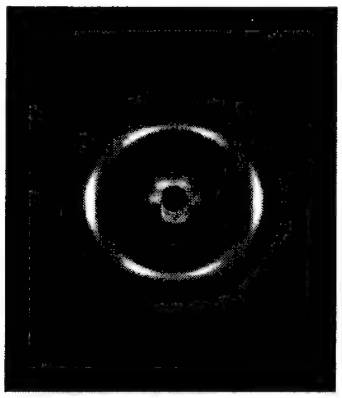

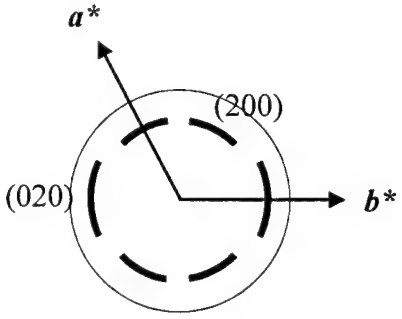

(b) Edge Mode

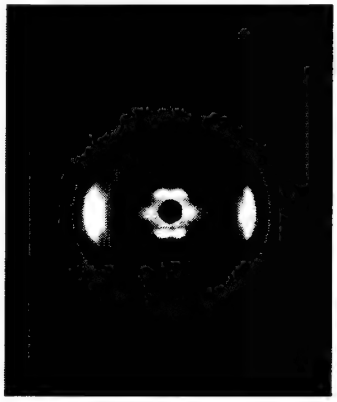

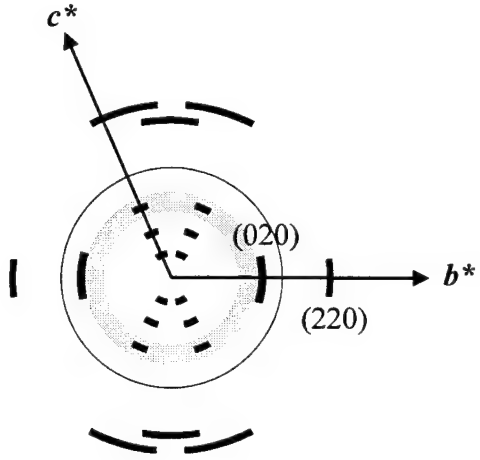

(c) Transmission Mode

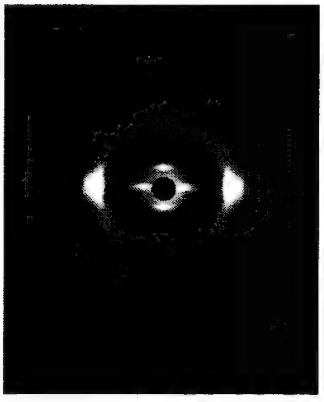

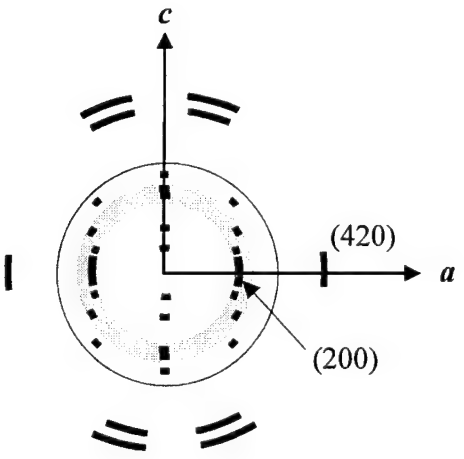

Figure 4 Flat plate wide-angle x-ray diffraction patterns of uniaxially drawn-annealed nylon 11 films with time in the melt of 30 s, along with the schematic representations of the observed reflections indexed according to Hasegawa's unit cell. (a) End mode, (b) Edge mode, and (c) Transmission mode.

(a) End Mode

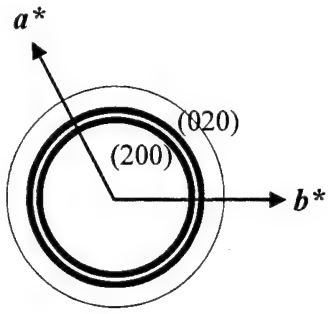

(b) Edge Mode

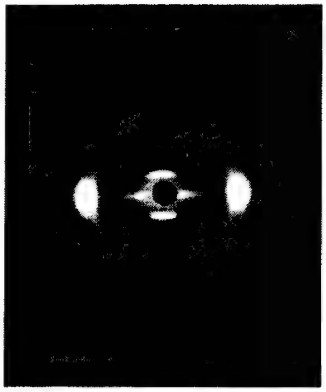

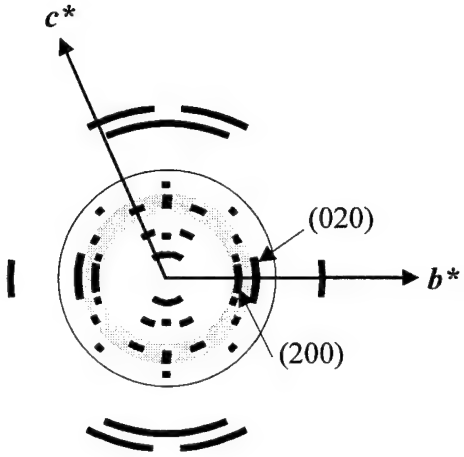

(c) Transmission Mode

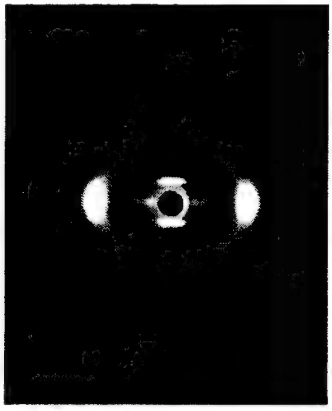

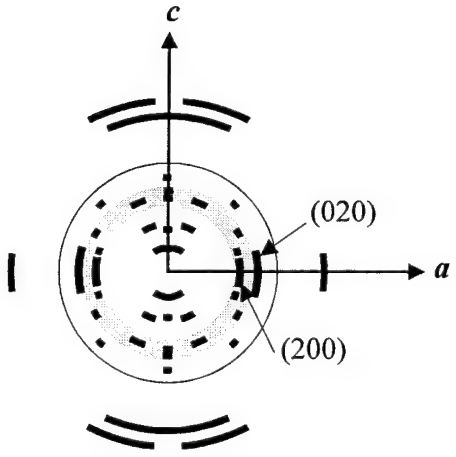

Figure 5 Flat plate wide-angle x-ray diffraction patterns of uniaxially drawn-annealed nylon 11 films with time in the melt of 10 m, along with the schematic representations of the observed reflections indexed according to Hasegawa's unit cell. (a) End mode, (b) Edge mode, and (c) Transmission mode.

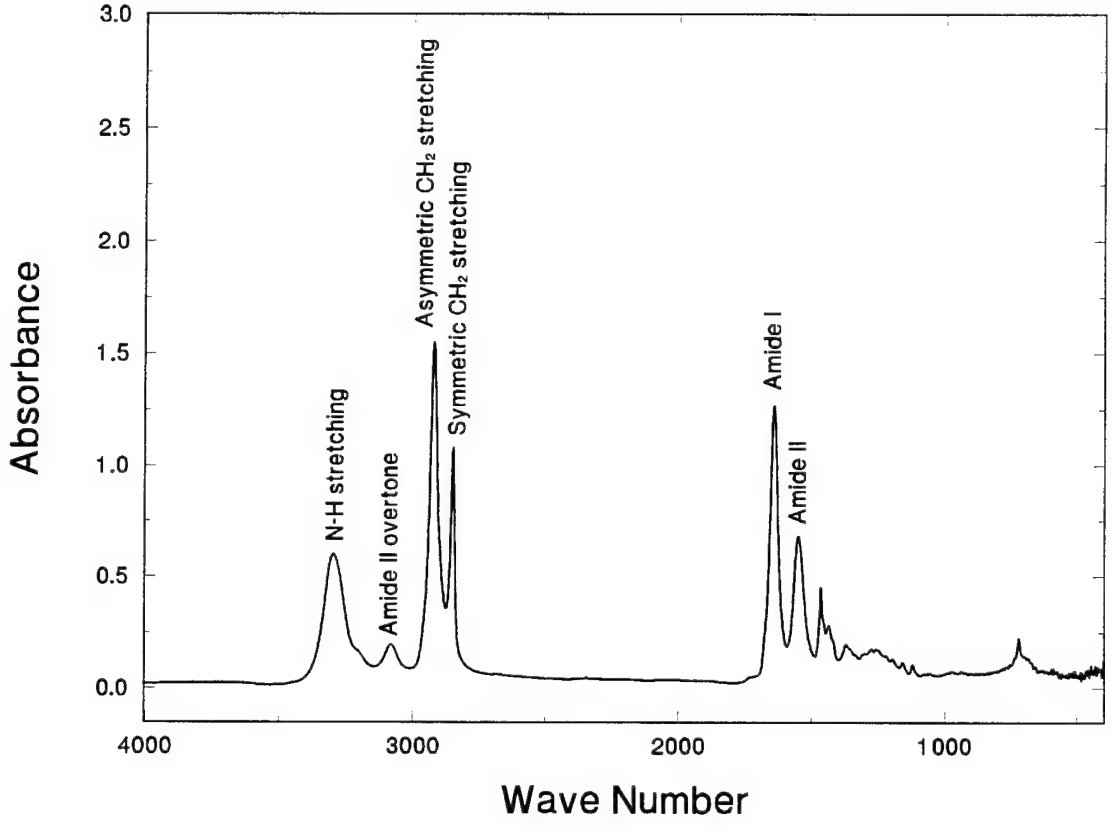

Figure 6 Typical FTIR spectrum for nylon 11 film.

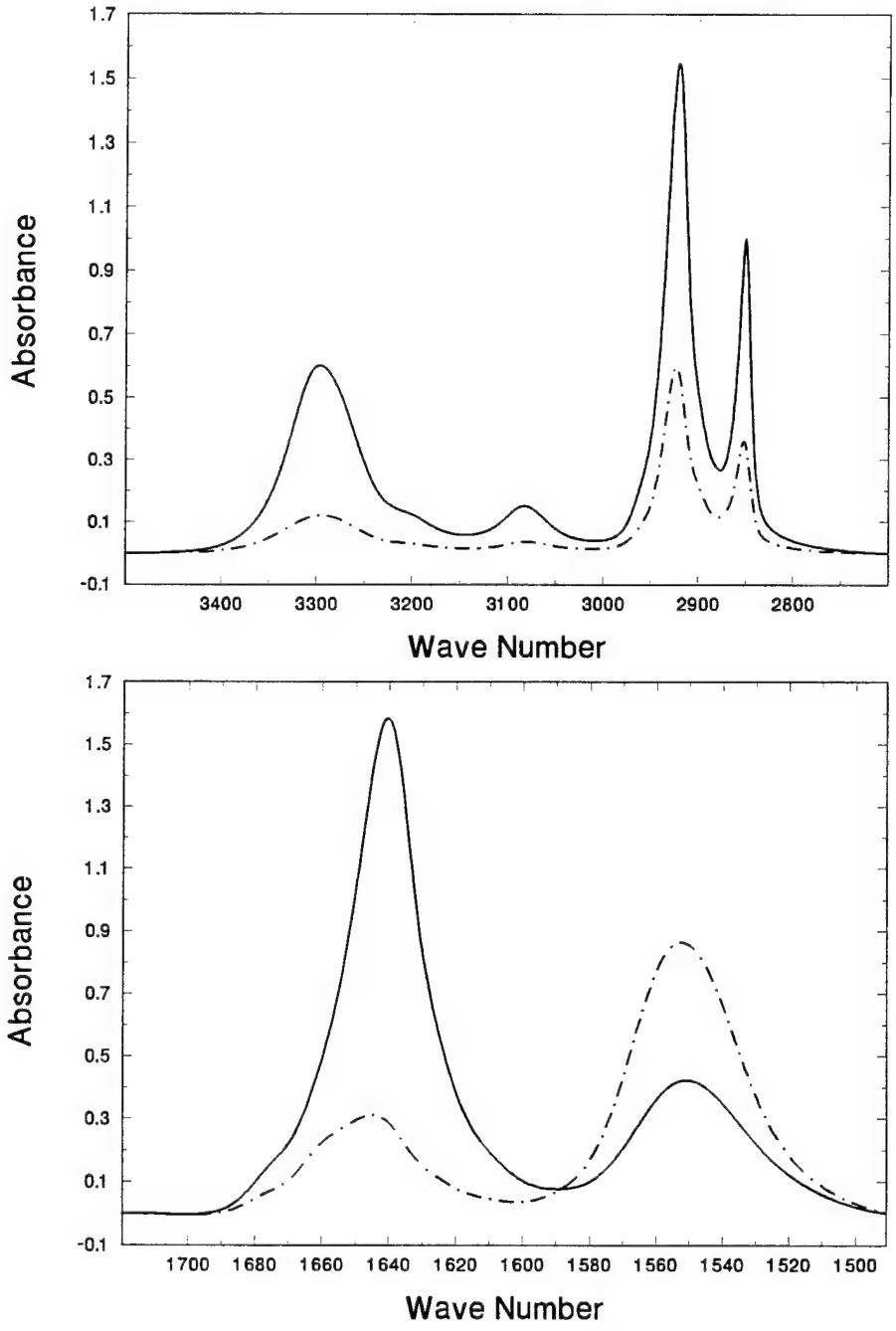

Figure 7 The drawing effect on melt-quenched nylon 11 films with time in the melt of 30 s. (a) shows N-H and CH_2 stretching bands and (b) shows Amide I and Amide II bands. The spectra with the polarizer in the parallel and perpendicular directions to the draw direction are shown in dot-dash and solid lines respectively.

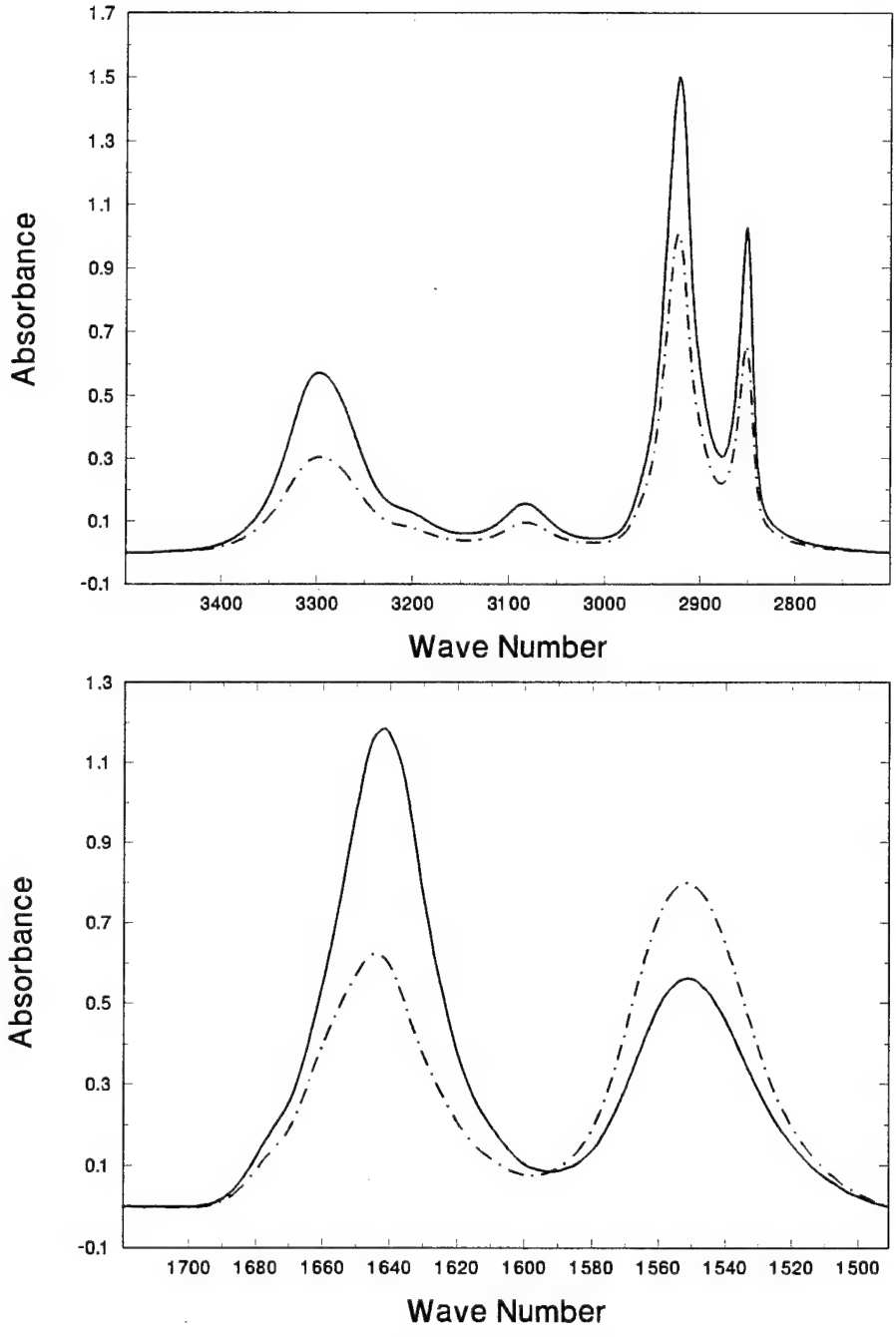

Figure 8 The drawing effect on melt-quenched nylon 11 films with time in the melt of 10 m. (a) shows N-H and CH_2 stretching bands and (b) shows Amide I and Amide II bands. The spectra with the polarizer in the parallel and perpendicular directions to the draw direction are shown in dot-dash and solid lines respectively.

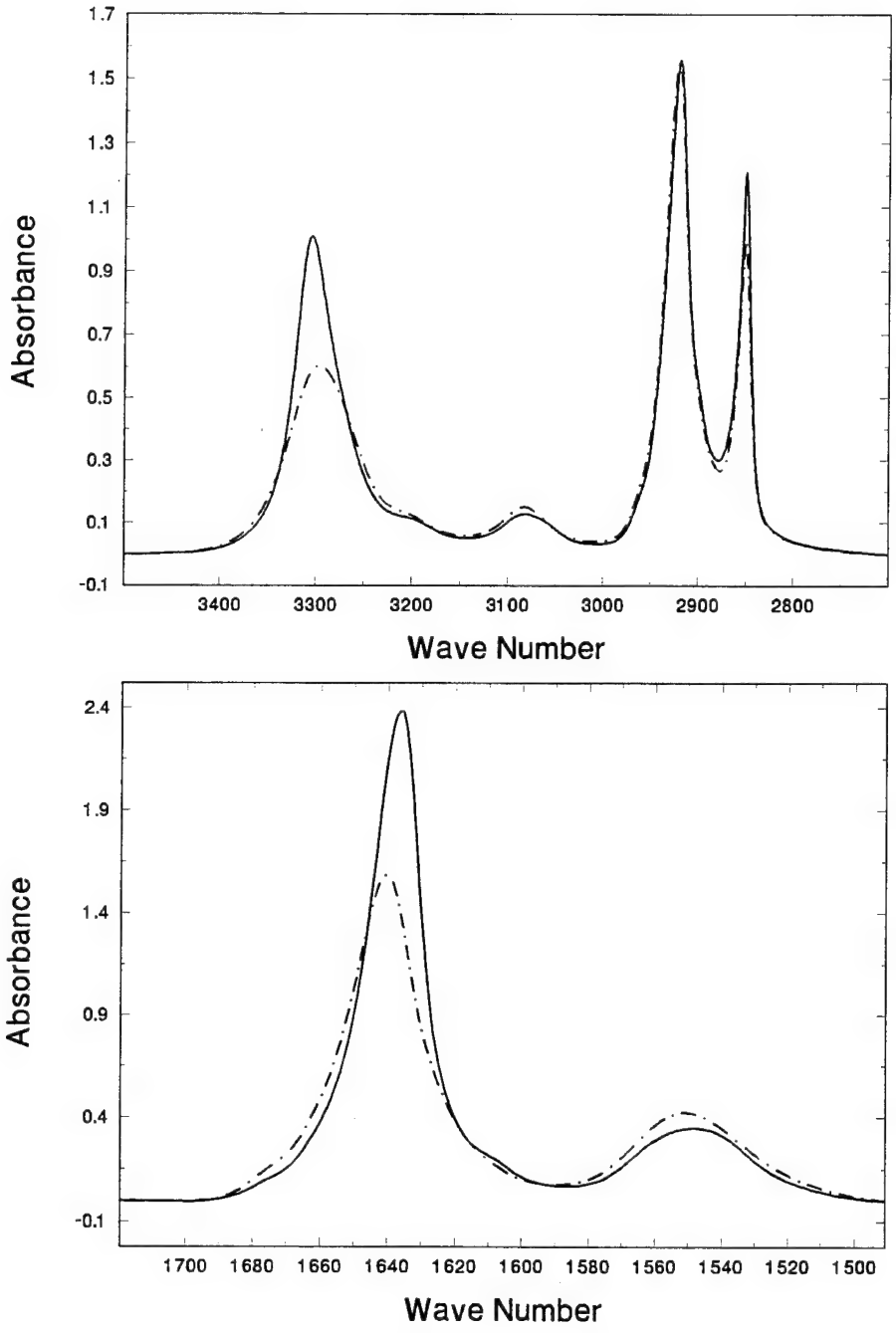

Figure 9 The effect of annealing on uniaxially drawn nylon 11 films with time in the melt of 30 s. (a) shows N-H and CH_2 stretching bands and (b) shows Amide I and Amide II bands with the polarizer in the direction perpendicular to the chain axis. The dot-dash and solid lines represent before and after annealing, respectively.

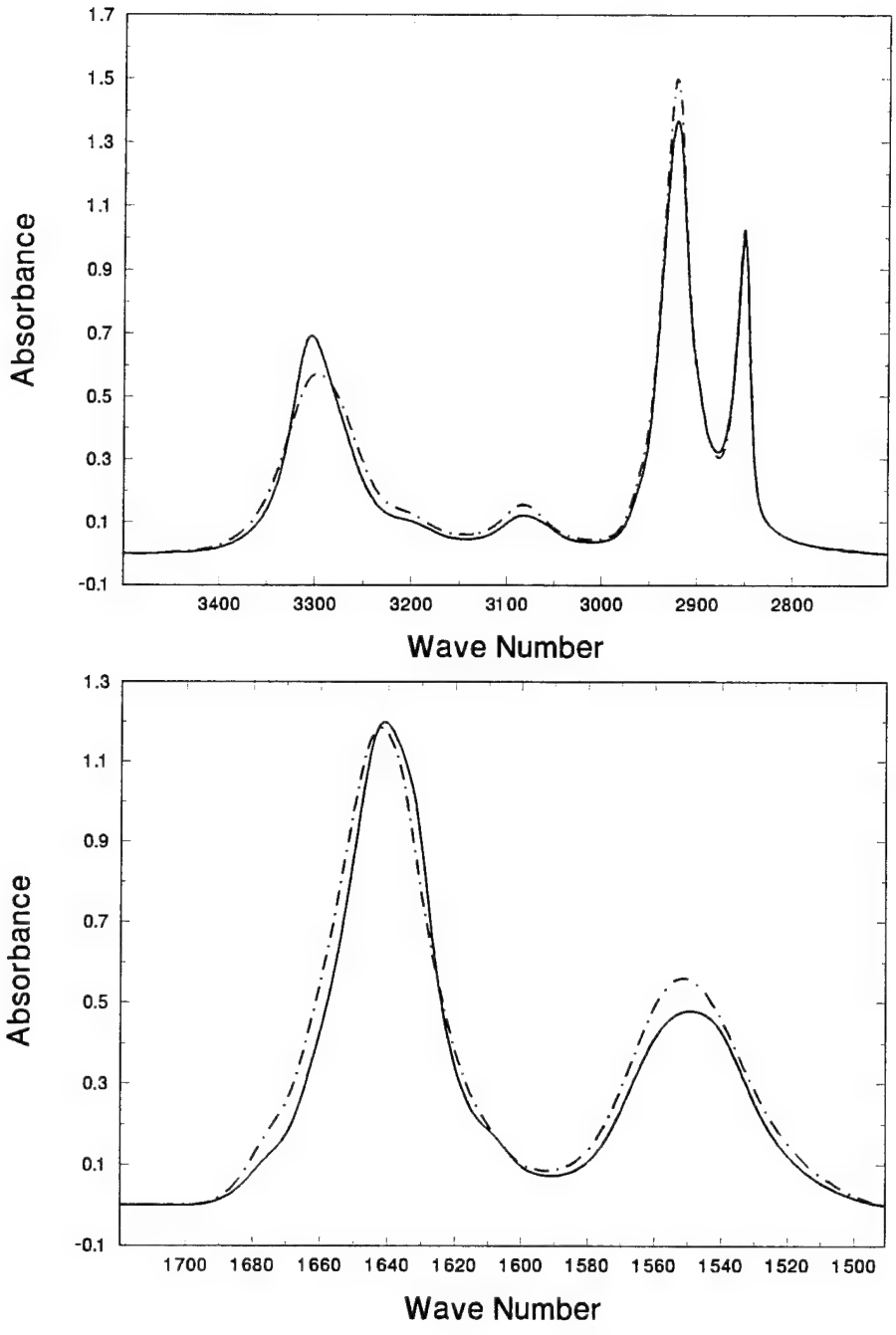

Figure 10 The effect of annealing on uniaxially drawn nylon 11 films with time in the melt of 10 m. (a) shows N-H and CH_2 stretching bands and (b) shows Amide I and Amide II bands with the polarizer in the direction perpendicular to the chain axis. The dot-dash and solid lines represent before and after annealing, respectively.

(a) Edge (or End) Mode

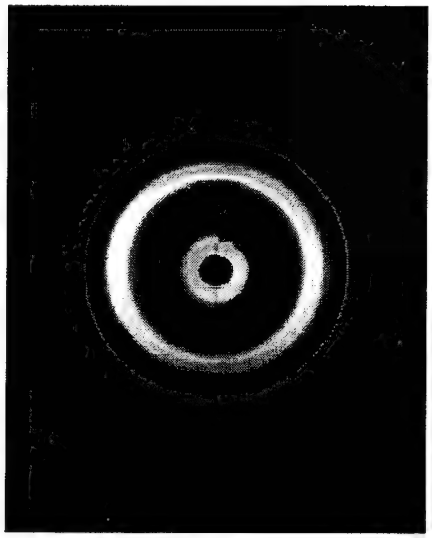

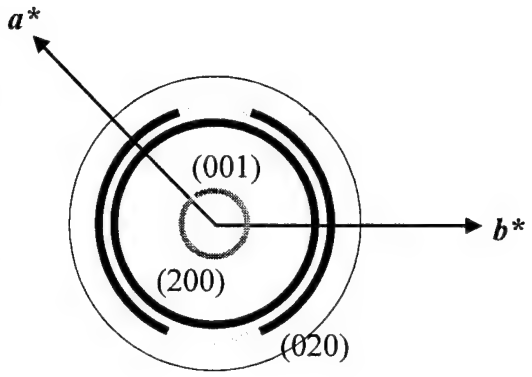

(b) Transmission Mode

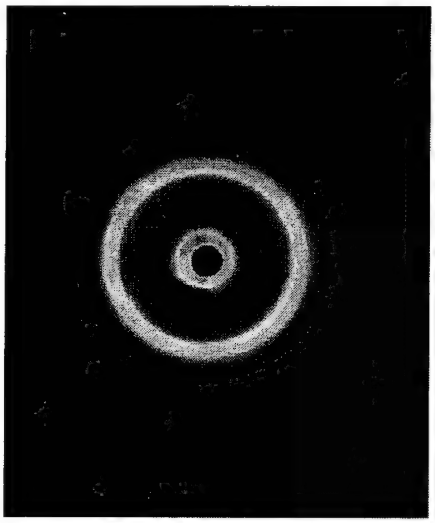

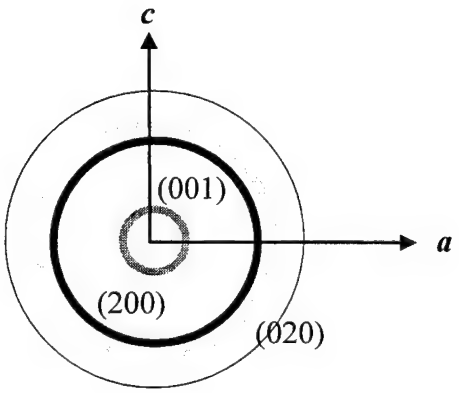

Figure 11 Flat plate wide-angle x-ray diffraction patterns of undrawn-annealed nylon 11 films with time in the melt of 30 s, along with the schematic representations of the observed diffraction patterns indexed according to Hasegawa's unit cell. (a) Edge (or End) mode, and (b) Transmission mode.

(a) Edge (or End) Mode

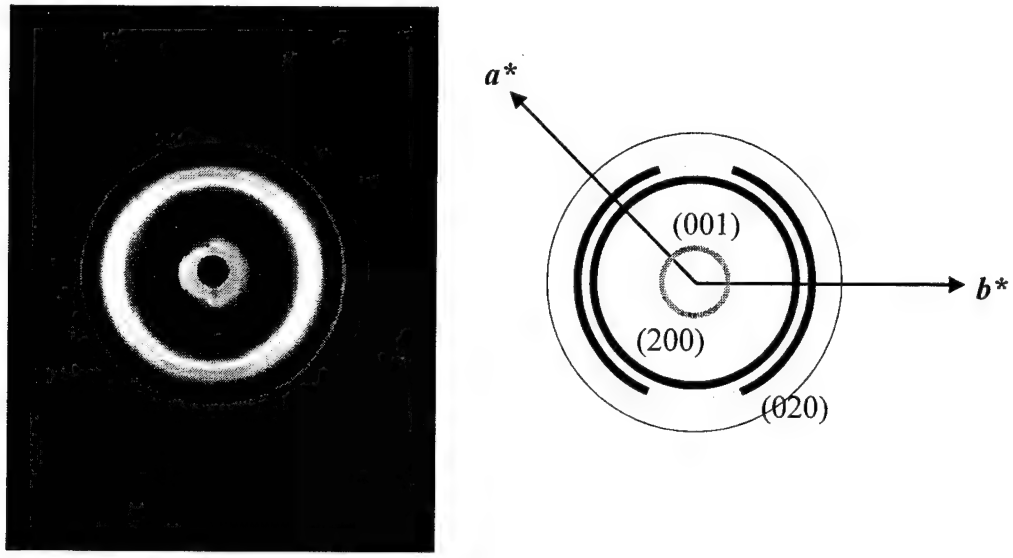

(b) Transmission Mode

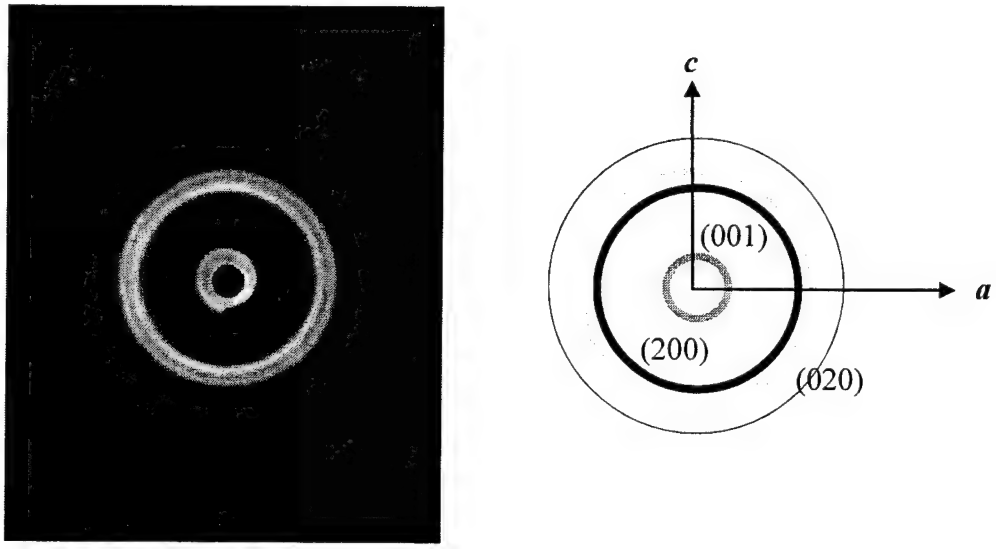

Figure 12 Flat plate wide-angle x-ray diffraction patterns of undrawn-annealed nylon 11 films with time in the melt of 10 m, along with the schematic representations of the observed diffraction patterns indexed according to Hasegawa's unit cell. (a) Edge (or End) mode, and (c) Transmission mode.

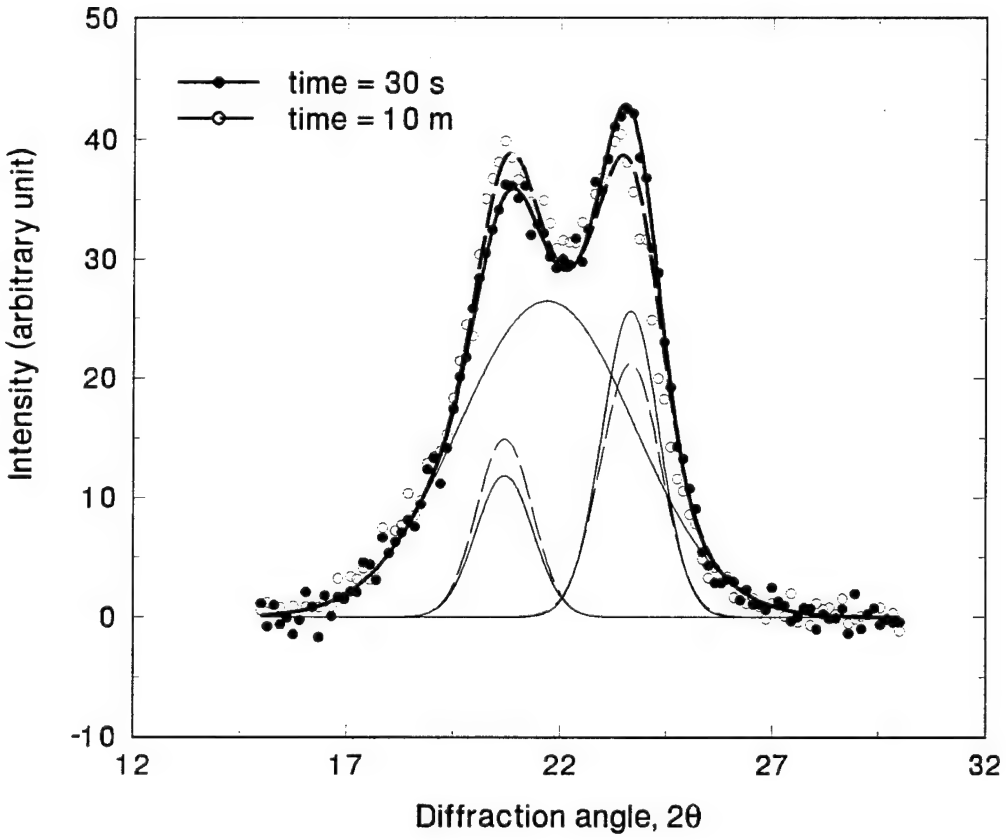

Figure 13 Wide-angle x-ray diffraction scans for undrawn-annealed nylon 11 films with times in the melt of 30 s and 10 m. The scans were taken in reflection mode. Each diffraction scan is curve fitted and area percentages of the (200) and (020) reflections were calculated and are shown in Table II.

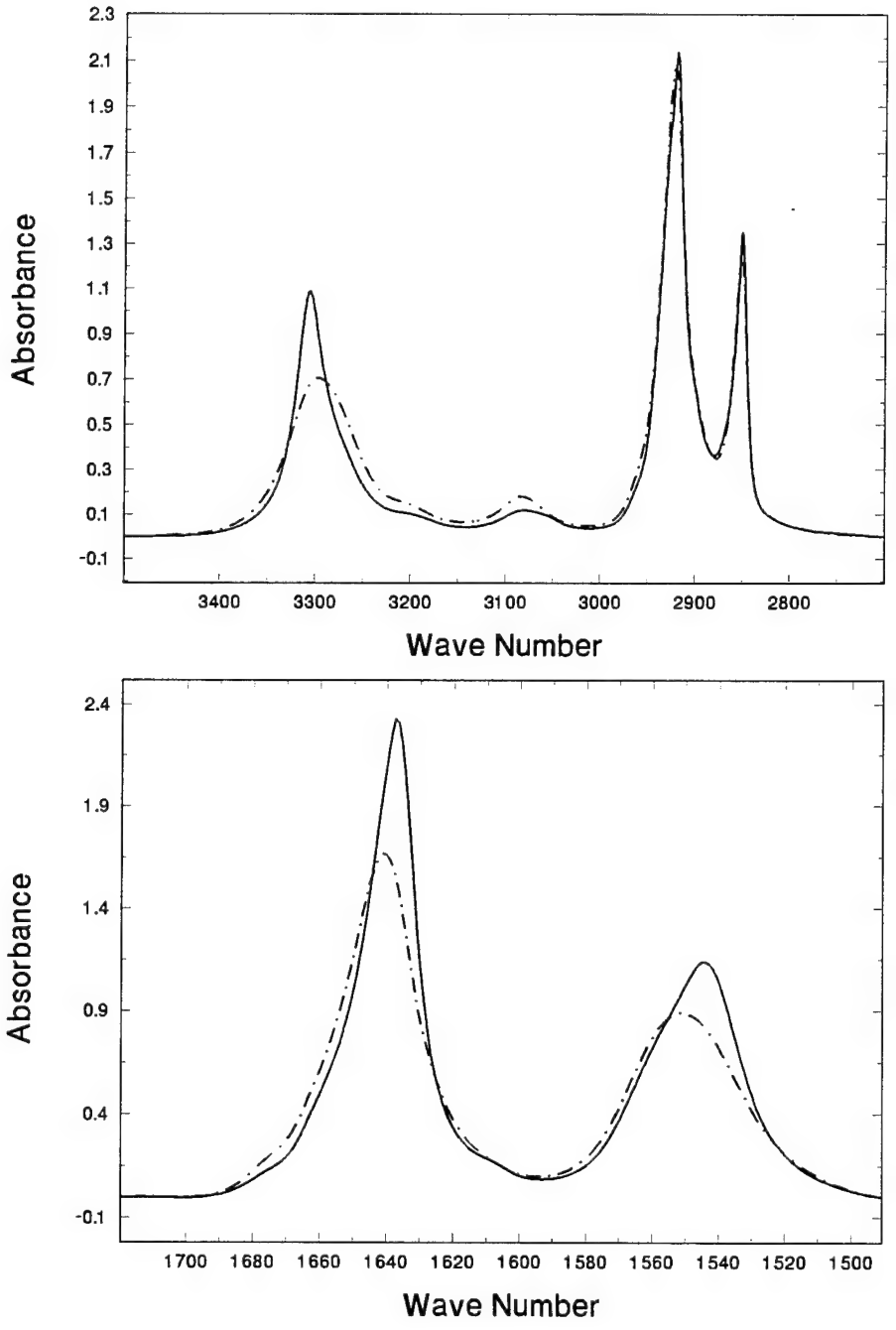

Figure 14 The IR spectra show the effect of annealing on undrawn nylon 11 films with time in the melt of 30 s. (a) shows N-H and CH_2 stretching bands and (b) shows Amide I and Amide II bands. The dot-dash and solid lines represent before and after annealing, respectively.

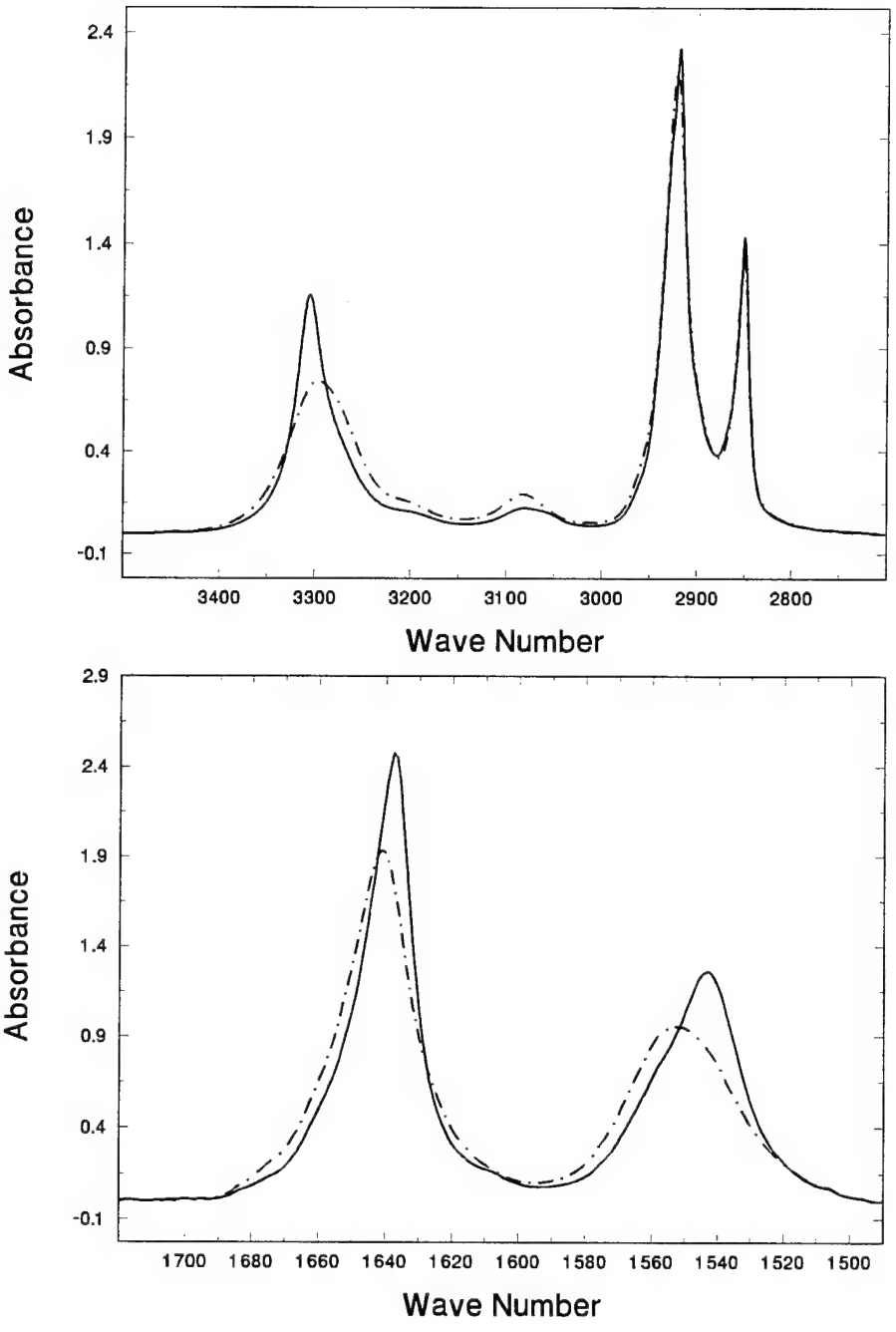

Figure 15 The IR spectra show effect of annealing on undrawn nylon 11 films with time in the melt of 10 m. (a) shows N-H and CH_2 stretching bands and (b) shows Amide I and Amide II bands. The dot-dash and solid lines represent before and after annealing, respectively.

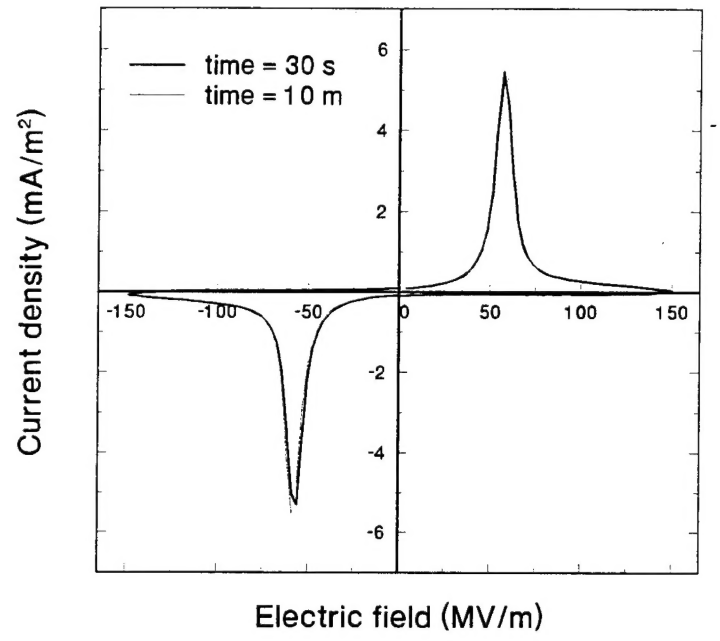

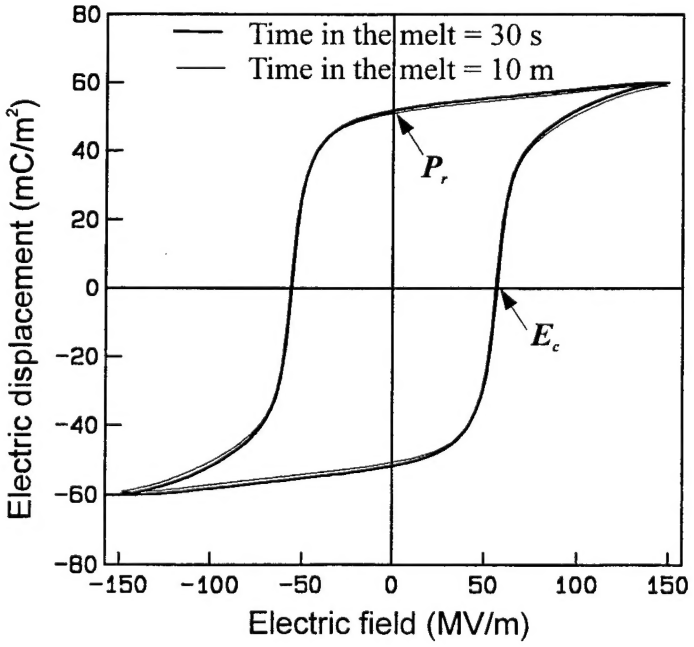

Figure 16 (a) shows current density, $\boldsymbol{J}$, and (b) shows electric displacement, $\boldsymbol{D}$, as a function of electric field, $\boldsymbol{E}$, respectively for uniaxially drawn nylon 11 films made from films with times in the melt of 30 s and 10 m.

(a) End Mode

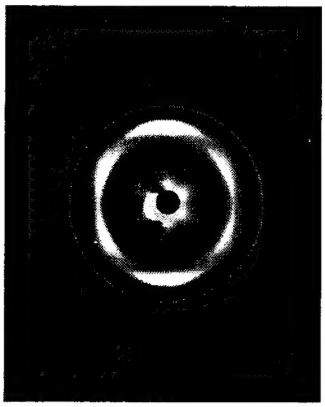

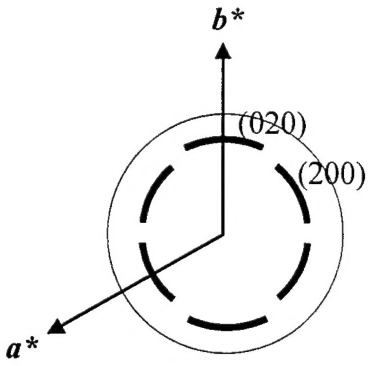

(b) Edge Mode

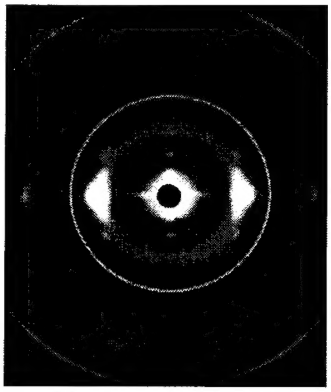

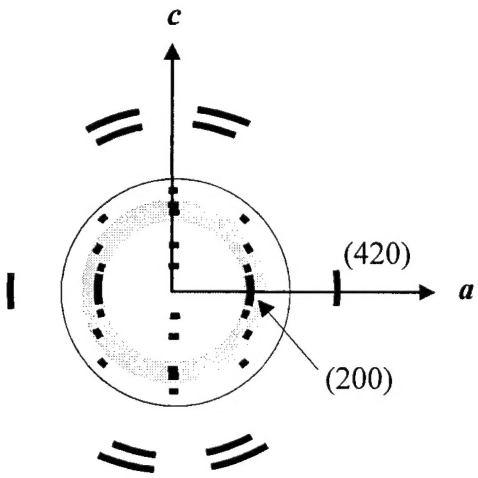

(c) Transmission Mode

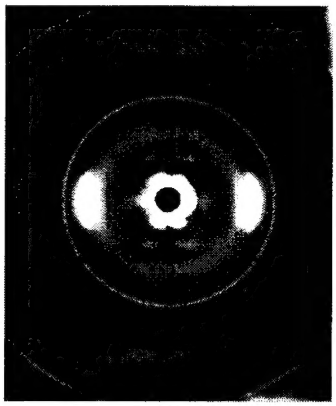

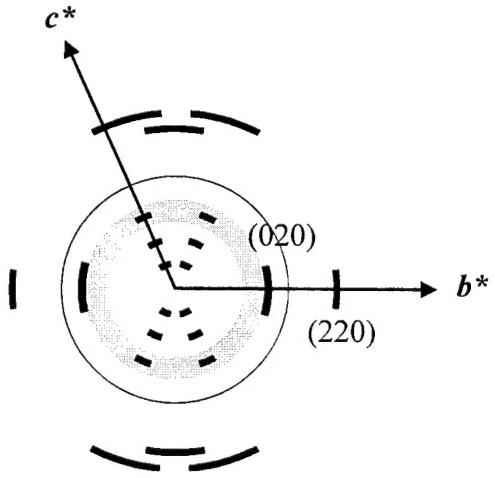

Figure 17 Flat plate wide-angle x-ray diffraction patterns of uniaxially drawn-poled-annealed nylon 11 films with time in the melt of 30 s, along with the schematic representations of the observed diffraction patterns indexed according to Hasegawa's unit cell. (a) End mode, (b) Edge mode, and (c) Transmission mode.

(a) End Mode

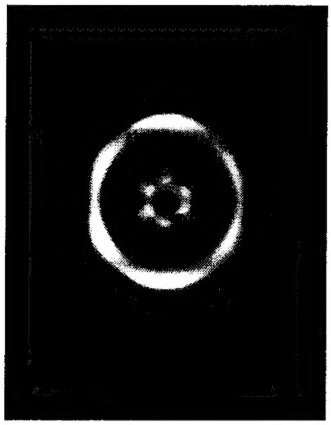

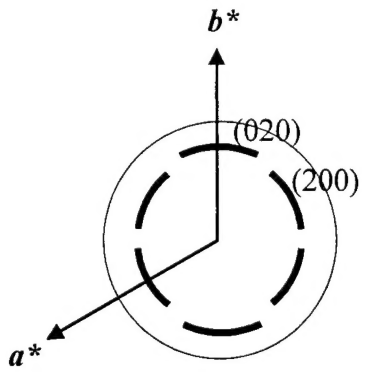

(b) Edge Mode

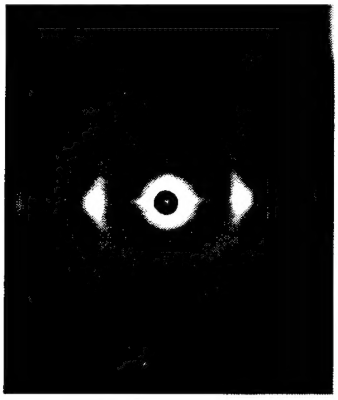

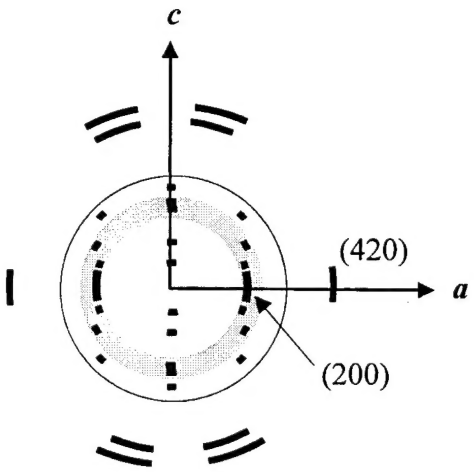

(c) Transmission Mode

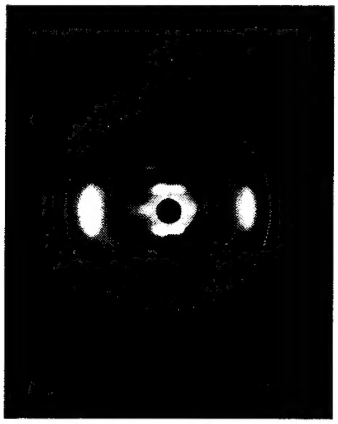

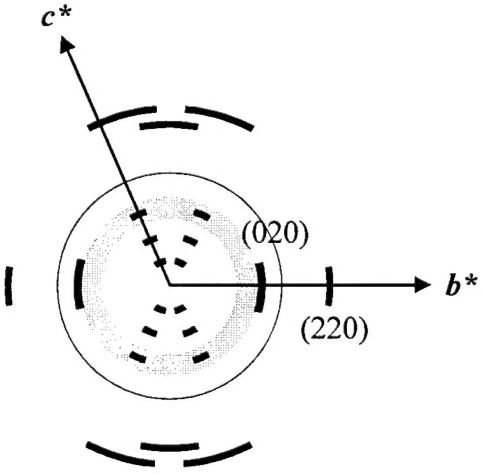

Figure 18 Flat plate wide-angle x-ray diffraction patterns of uniaxially drawn-poled-annealed nylon 11 films with time in the melt of 10 m, along with the schematic representations of the observed diffraction patterns indexed according to Hasegawa's unit cell. (a) End mode, (b) Edge mode, and (c) Transmission mode.

Reference

[1] J.W. Lee, Y. Takase, B.A. Newman, and J.I. Scheinbeim, *J. Polym. Sci. Part B: Poly. Phys.*, **29**, 273 (1991).

[2] B.Z. Mei, J.I. Scheinbeim, and B.A. Newman, *Ferroelectrics*, **144**, 51 (1993).

[3] Y. Takase, J.W. Lee, J.I. Scheinbeim, and B.A. Newman, *Macromolecules*, **24**, 6644 (1991).

[4] M.G. Northolt, *J. Poly. Sci. Part C*, **38**, 205 (1972).

[5] J.I. Scheinbeim, J.W. Lee, and B.A. Newman, *Macromolecules,* **25**, 3729 (1992).

[6] G.A. Gordon, presented at IUPAC Symposium, Abstract III 49, Leiden, Netherlands, (1970).

[7] R.K. Hasegawa, K. Kimoto, Y. Chatani, H. Tadokoro and H. Sekiguchi, *Discussion Meeting of the Society of Polymer Science,* Japan, Tokyo, Preprint, 713 (1974).

[8] E.S. Clark and F.C. Wilson, *Nylon Plastic*, chapter 8, John-Wiley & Sons (1973)

[9] H.H. Yu and L.J. Fina, *Macromolecules,* **27**, 6192 (1994).

[10] B.Z. Mei, Ph.D. Dissertation, Rutgers University (1994).

[11] W.H. Moore and S. Krimm, *Biopolymers*, **15**, 2439 (1976).

[12] T. Miyazawa, *J. Chem. Phys.,* **32(6)**, 1647 (1960).

[13] D.J. Skrovanek, P.C. Painter, and M.M. Coleman, *Macromolecules,* **19**, 699 (1986)

[14] J.W. Lee, Y. Takase, B.A. Newman, and J.I. Scheinbeim, *J. Poly. Sci. Part B: Poly. Phys.*, **29**, 279 (1991).

[15] E. Bessler and G. Bier, *Macromol. Chem.*, **122**, 30 (1969).

[16] T. Itoh, *Jpn. J. Appl. Phys.*, **15**, 2295 (1976).

[17] B.Z. Mei, J.I. Scheinbeim, and B.A. Newman, *Ferroelectrics*, **171**, 177, (1995).